Electronic Supplementary Material (ESI) for Chemical Science

Supporting Information

Solid-state structural transformation doubly triggered by reaction temperature and time in 3D metal–organic frameworks: great enhancement of stability and gas adsorption

Ping Shen,[a] Wen-Wen He,[a] Dong-Ying Du,[a] Hai-Long Jiang,[c] Shun-Li Li,[b] Zhong-Ling Lang,[a] Zhong-Min Su,*[a] Qiang Fu,[a] and Ya-Qian Lan*[a,b]

[a] Institute of Functional Material Chemistry, Department of Chemistry, National & Local United Engineering Lab for Power Battery, Northeast Normal University, Changchun 130024, P. R. China

[b] Jiangsu Key Laboratory of Biofunctional Materials, College of Chemistry and Materials Science, Nanjing Normal University, Nanjing 210023, P. R. China

[c] Hefei National Laboratory for Physical Sciences at the Microscale, Department of Chemistry, University of Science and Technology of China, Hefei 230026, P. R. China

Corresponding Author: zmsu@nenu.edu.cn; yqlan@njnu.edu.cn

S1. Materials and instrumentations for measurements

Tetrakis[4-(carboxyphenyl)oxamethyl]methane acid (H_4L) was synthesized according to the published procedures.[1] All of the chemical materials were purchased and used without further purification. The FT-IR spectra were recorded from KBr pellets in the range 4000-400 cm^{-1} on a Mattson Alpha-Centauri spectrometer. The C, H, and N elemental analyses were conducted on a Perkin-Elmer 240C elemental analyzer. The phase purities of the bulk samples were identified by X-ray powder diffraction on a Rigaku, Rint 2000 diffractometer. TGA was measured on a Perkin–Elmer TG-7 analyzer heated from room temperature to 1000 ºC at a ramp rate of 5 °C/min under nitrogen. The photoluminescence spectra were performed on a Perkin-Elmer FLS-920 Edinburgh Fluorescence Spectrometer. The N_2, H_2 and CO_2 sorption measurements were performed on an automatic volumetric adsorption equipment (Belsorp mini II). Before gas adsorption measurements, the sample was immersed in methanol for 24 h, and the liquid was poured out. Fresh methanol was added subsequently, and the crystals were stay for an additional 24 h to remove the nonvolatile solvates (DMF). The extract was decanted and fresh methanol was added once more. The sample was collected by decanting and treated with dichloromethane similarly to remove methanol solvates. After the removal of dichloromethane by decanting, the sample was activated by drying under a dynamic vacuum at room temperature overnight. Before the measurement, the sample was dried again by using the 'outgas' function of the surface area analyzer for 12 h at room temperature.

S2. Single-crystal X-ray diffraction

Single-crystal X-ray diffraction data for **IFMC-68** and **IFMC-69** were recorded by using a Bruker Apex CCD diffractometer with graphite-monochromated Mo-Kα radiation (λ = 0.71069 Å) at 293 K. Absorption corrections were applied by using a multi-scan technique. All the structures were solved by the direct method of SHELXS-97[2] and refined by full-matrix least-squares techniques using the SHELXL-97 program within WINGX[3]. Non-hydrogen atoms were refined with anisotropic temperature parameters. Contributions to scattering due to these solvent molecules were removed using the SQUEEZE routine of PLATON[4]; structures were then refined again using the data generated. The detailed crystallographic data and structure refinement parameters for **IFMC-68** and **IFMC-69** are summarized in article.

S3. Electrical conductivity values (σ) of IFMC-69 and I_2@IFMC-69

A bulk sample of colorless crystals of **IFMC-69** was washed with anhydrous methanol (3×50 mL), and then the crystals were soaked for 24 h. Then the crystals were similarly washed three times with dichloromethane (3×50 mL)-again, and crystals were soaked for 24 hours before the dichloromethane was decanted. The solvent was decanted after the final dichloromethane wash, and the resultant crystals were evacuated with an oil pump at 45 °C for 2 hours to give 0.9 g of **IFMC-69**. Half of the activated **IFMC-69** were immersed in the hexane solution of I_2 (0.05 mol/L) for 24 hours,

and then were evacuated with an oil pump at 45 °C for 2 hours to give 0.49 g of activated **I_2@IFMC-69**. Then the activated **IFMC-69** and **I_2@IFMC-69** were grinded to powder and pressed into a 1 mm thickness film respectively. Square resistances are 3.57×10^5 Ω for **I_2@IFMC-69** and 8.00×10^{13} Ω for **IFMC-69**, respectively. Converted into electrical conductivity, the values (σ) are 2.80×10^{-6} S/cm for **I_2@IFMC-69** which is in the semiconductor range and 1.25×10^{-13} S/cm for **IFMC-69**, respectively.

References:

[S1] D. Laliberte, T. Maris and J. D. Wuest, *J. Org. Chem*. 2004, **69**, 1776.

[S2] G. M. Sheldrick, SHELXS-97, Programs for X-ray Crystal Structure Solution University of Göttingen: Göttingen, Germany, 1997.

[S3] L. J. Farrugia, WINGX, A Windows Program for Crystal Structure Analysis University of Glasgow: Glasgow, U.K., 1988.

[S4] A. L. Spek and J. Appl, *Crystallogr*., 2003, **36**, 7.

S4. Figures in Supporting Information

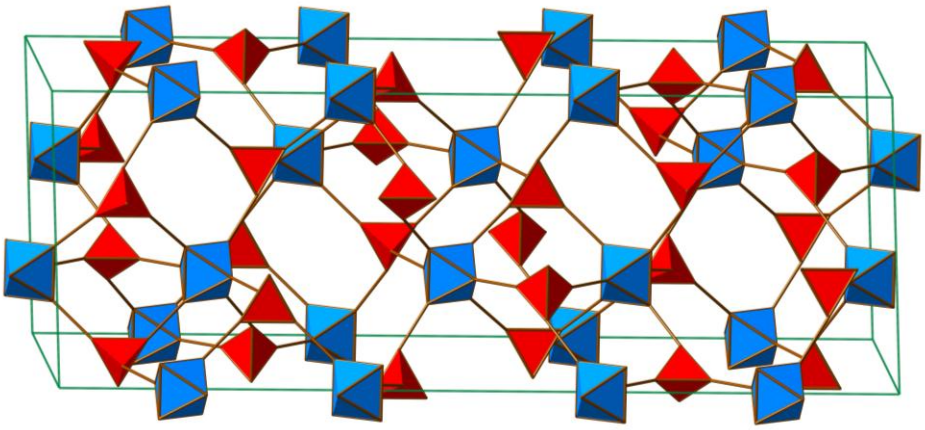

Fig. S1 The 3D (4,6)-connected topological net of **IFMC-68**, and the entire MOF framework is an ideal corundum structure.

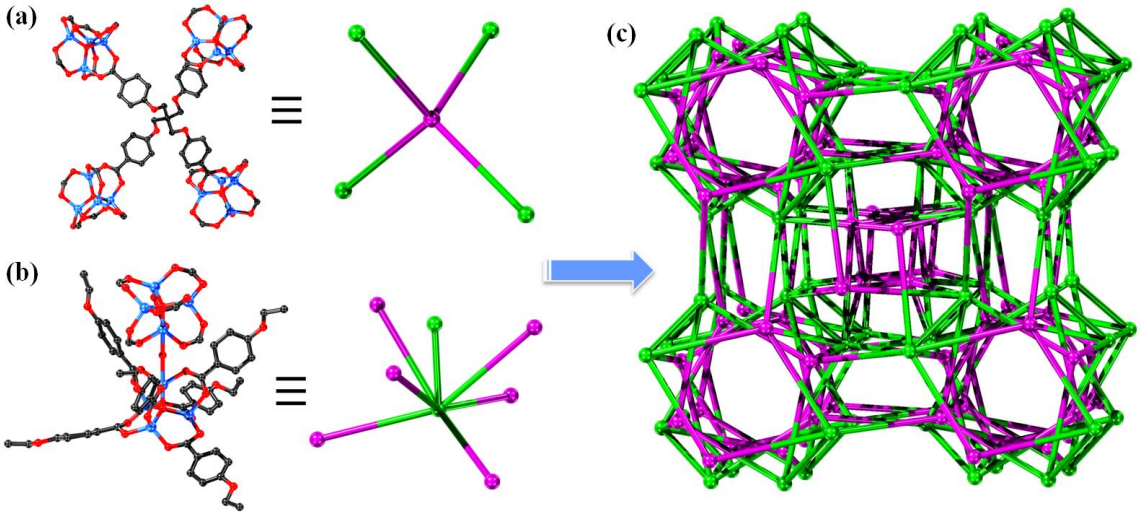

Fig. S2 (a) and (b) The ball-and-stick and topological representations of the 4-connected and 7-connected nodes. (c) Schematic representation of the 3D (4,7)-connected topological net of **IFMC-69**.

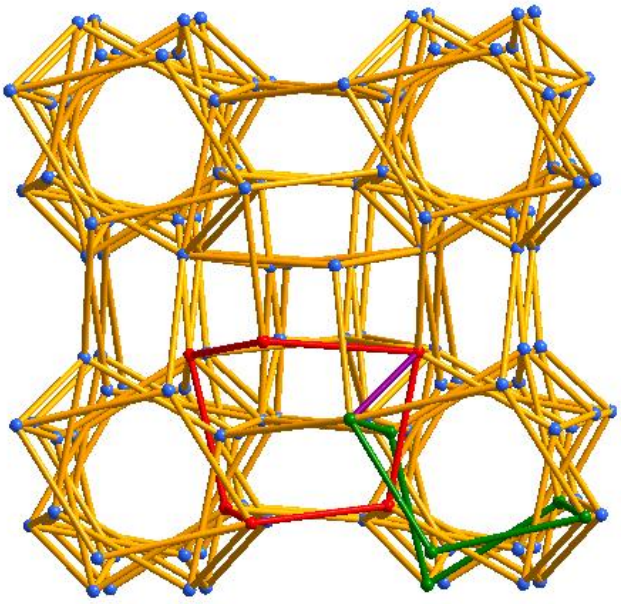

Fig. S3 The purple linker connection with the interpenetrated rings (in red and green) to from the self-penetrated structure of the 3D (4,7)-connected topological net in **IFMC-69**.

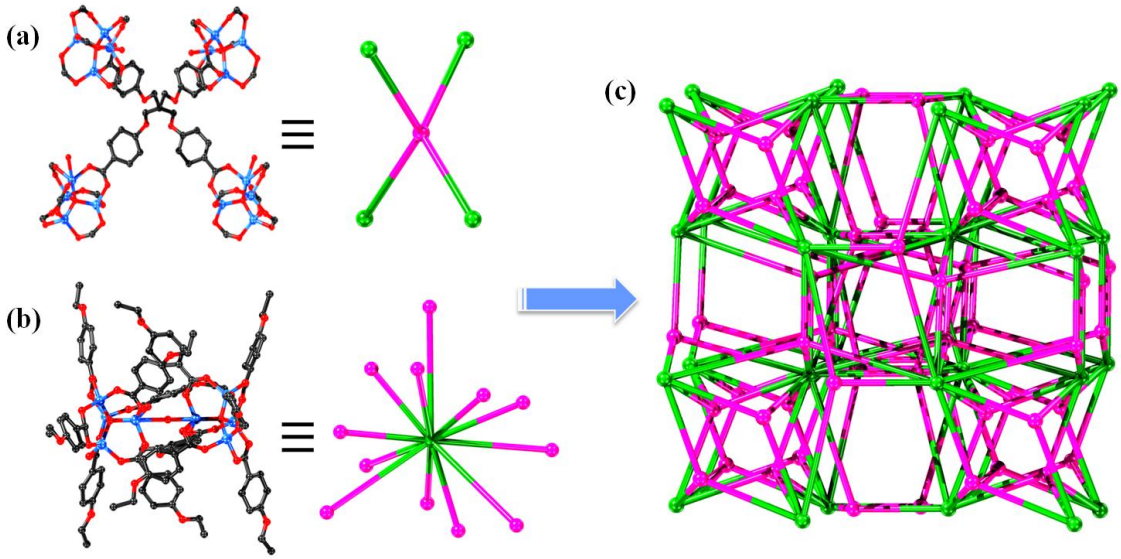

Fig. S4 (a) and (b) The ball-and-stick and topological representations of the 4-connected and 12-connected nodes. (c) Schematic representation of the 3D (4,12)-connected topological net of **IFMC-69**

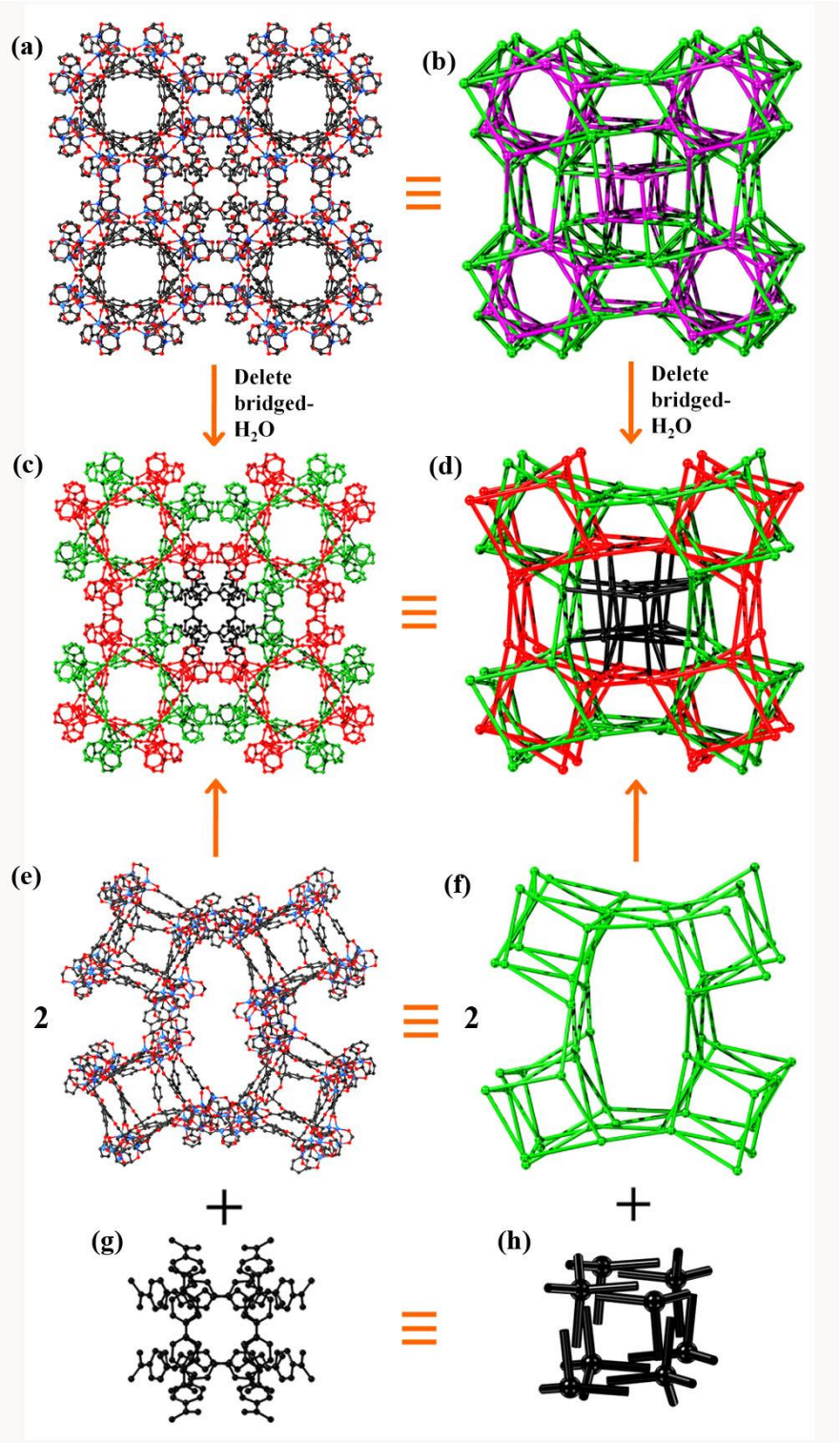

Fig. S5 (a) A ball-and-stick view of the 3D structure of **IFMC-69**. (b) The (4,7)-connected topological net of **IFMC-69**. (c) The ball-and-stick representation of the 3D structure of **IFMC-69** without the coordination water molecules. (d) The (4,6)-connected topological net of **IFMC-69** without the coordination water molecules. (e)-(h) The ball-and-stick and topological representations of two kinds of parts for **IFMC-69**.

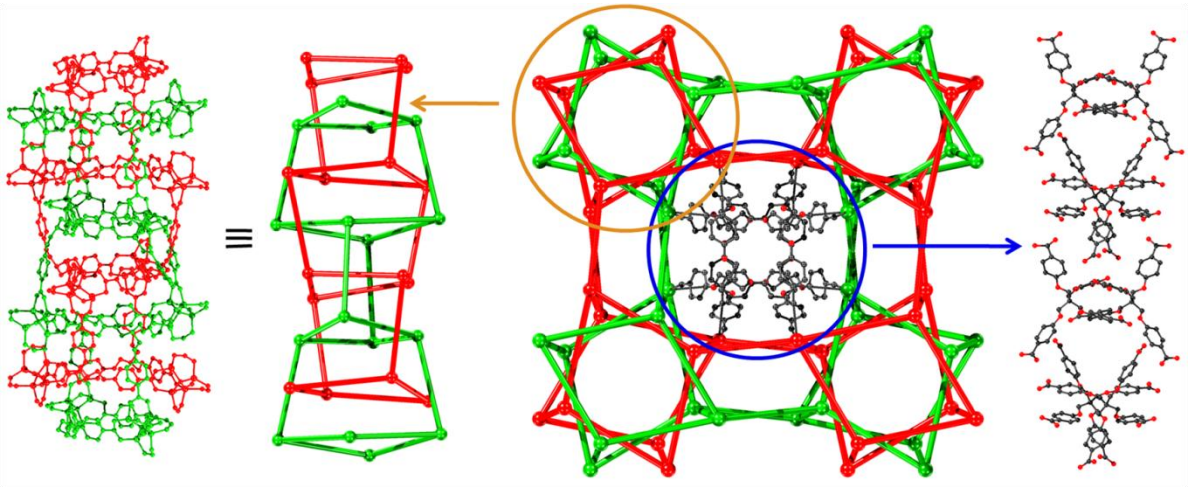

Fig. S6 The ball-stick and schematic view of the 1D channel in **IFMC-69** along the *b* axis (left) without the coordination water molecules. Arrangement of the shared ligands along the *b* axis (right).

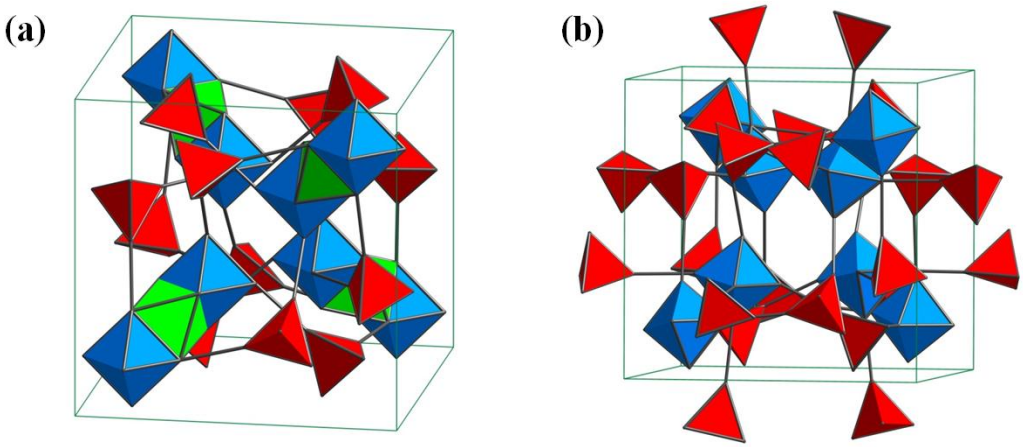

Fig. S7 The (4, 7)-connected topology of **IFMC-69** (a), and the (4,6)-connected topology of **IFMC-69** (b).

Neglecting the coordination water molecules of **IFMC-69**, it can be regarded as a (4,6)-connected structure. Looking at the augmented forms in which the vertices are the points of extension. For example, the C atoms of the linker tetrahedron and the carboxylate C atoms of the metal SBU are the vertices. The cubic (4,6)-connected net is exceptional in the extent of self-entanglement. It is also very dense, the topological density is TD_{10} = 3326, comparing the topological density for **IFMC-68** (TD_{10} = 1345). The short Schläfli symbol is $(4^2{\cdot}6^3{\cdot}8)_3{\cdot}(4^3{\cdot}6^6{\cdot}8^6)_2$, the long Schläfli symbol is $(4{\cdot}4{\cdot}6_2{\cdot}6_2{\cdot}6_4{\cdot}8_{10})_3{\cdot}(4{\cdot}4{\cdot}4{\cdot}6_2{\cdot}6_2{\cdot}6_2{\cdot}6_2{\cdot}6_2{\cdot}6_2{\cdot}8_3{\cdot}8_3{\cdot}8_3{\cdot}8_5{\cdot}8_5{\cdot}8_5)$. The relatively large subscripts show that the rings are very non-planar.

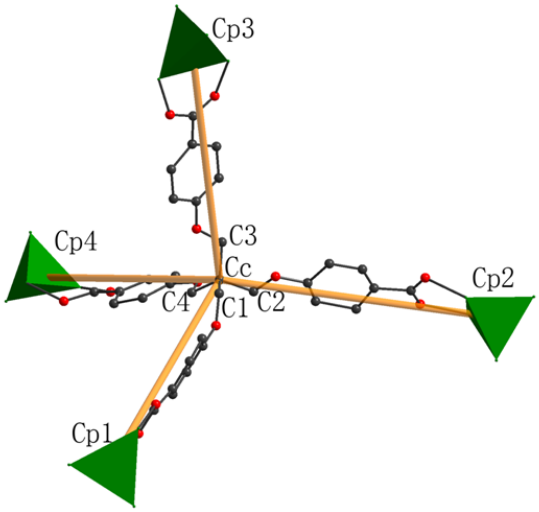

Angle	**IFMC-68** (°)	**IFMC-69** (°)
∠C1CcC2	106	105
∠C1CcC3	106	107
∠C1CcC4	111	109
∠C2CcC3	111	110
∠C2CcC4	112	111
∠C3CcC4	112	114
∠Cp1CcCp2	86	103
∠Cp1CcCp3	86	108
∠Cp1CcCp4	136	130
∠Cp2CcCp3	136	102
∠Cp2CcCp4	86	102
∠Cp3CcCp4	127	108

Scheme S1. The angles between ligand and Zn_4O cluster in **IFMC-68** and **IFMC-69**.

The distances between the center carbon atom in the ligand and the center of Zn_4O clusters are in the range from 11.35 to 11.39 Å for **IFMC-68**, and 11.19 to 11.30 Å for **IFMC-69**, respectively. It is obviously that the distances between the center carbon atom in the ligand and the center of Zn_4O clusters are changed after the SCSC transformation. As is shown in Table S2, the angles of $C_{1,2,3,4}$–Cc–$C_{1,2,3,4}$ have changed in 1-2º after the SCSC transformation. And the angles of Cp–Cc–Cp are in the range from 86 to 136 º for **IFMC-68**, and 102 to 130 º for **IFMC-69**. The different distances between the center carbon atom in the ligand and the center of Zn_4O cluster, and the different angles of Cp–Cc–Cp and $C_{1,2,3,4}$–Cc–$C_{1,2,3,4}$ result in the different conformations of the ligands in **IFMC-68** and **IFMC-69**. Therefore, we consider that the cooperative bond breakage, formation and the comformational change of the ligand lead to the different structure of **IFMC-68**

and **IFMC-69**. As is known to us, the angle of the centre tetrahedral geometrical conFigureuration is 109.28º. For **IFMC-68**, the four arms of the ligand are in a highly distorted tetrahedral orientation. For **IFMC-69**, the ligands also adopt a conformation that holds the four arms in a distorted tetrahedral orientation, it is closer to regular tetrahedral geometrical conFigureuration than that of **IFMC-68**.

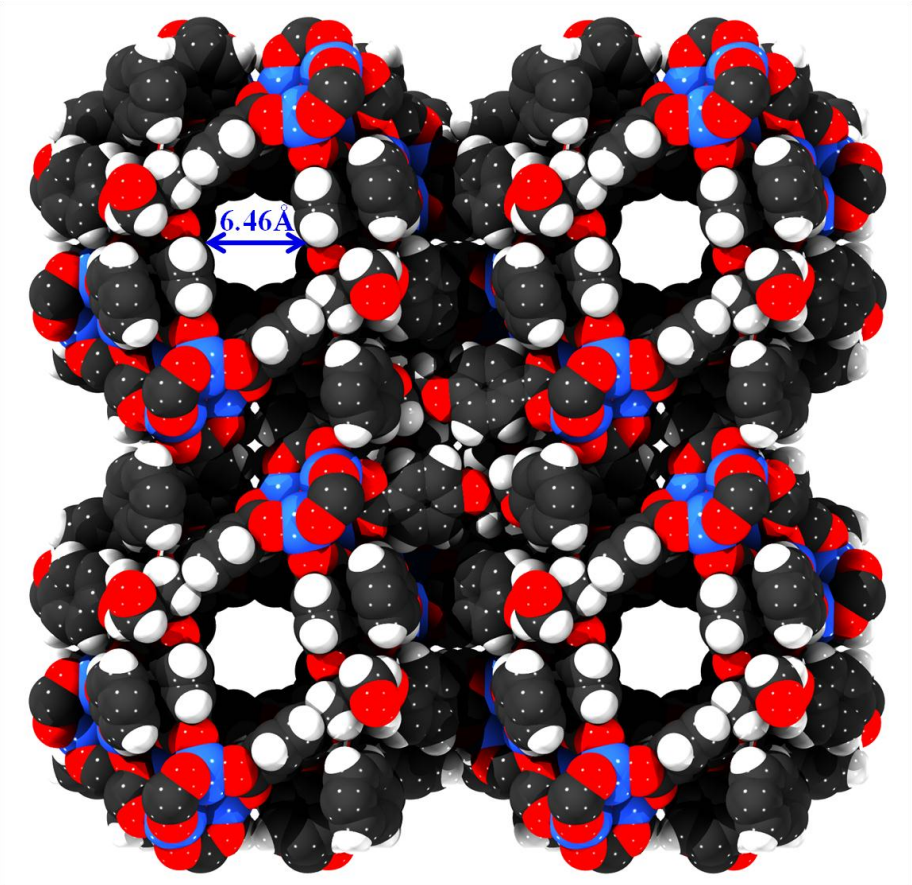

Fig. S8 Space-filling model of **IFMC-69** along the *c* axis and the channels with a diameter of 6.46 Å.

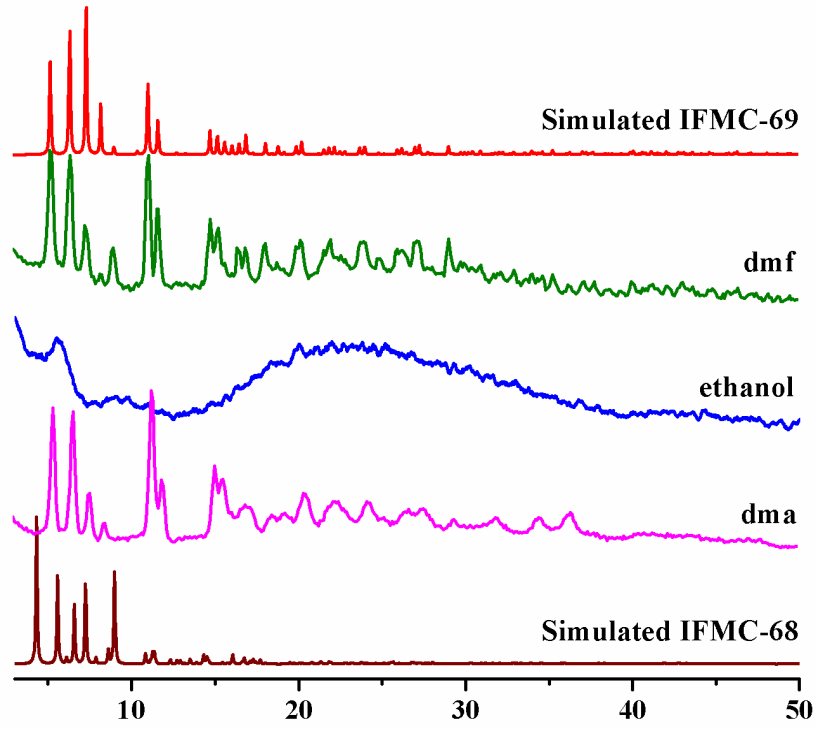

Fig. S9 X-Ray powder diffraction patterns of simulated **IFMC-68** (dark red), **IFMC-68** into a Teflon reactor with 5 mL solvent (DMA: pink, ethanol: blue, DMF: green) heated at 140℃, and simulated **IFMC-69** (red).

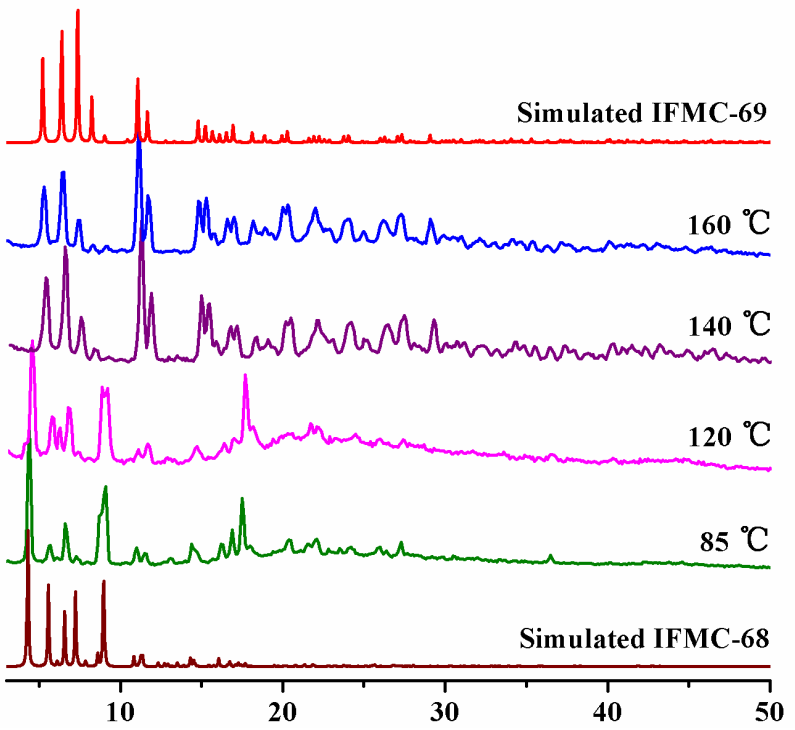

Fig. S10 X-Ray powder diffraction patterns of simulated **IFMC-68** (dark red), **IFMC-68** in a Teflon liner without solvent at 85℃ (green), 120℃ (pink), 140℃ (purple), 160℃ (blue) for 72 h, and simulated **IFMC-69** (red).

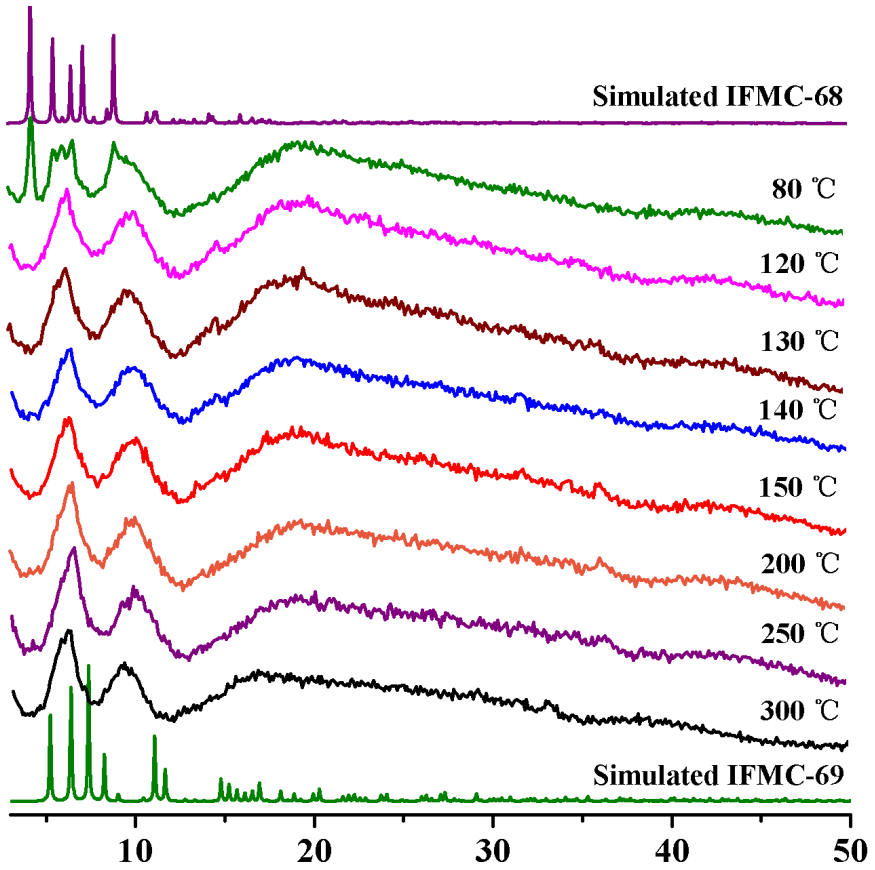

Fig. S11 Variable-temperature powder X-ray diffraction (VT-PXRD) of **IFMC-68**.

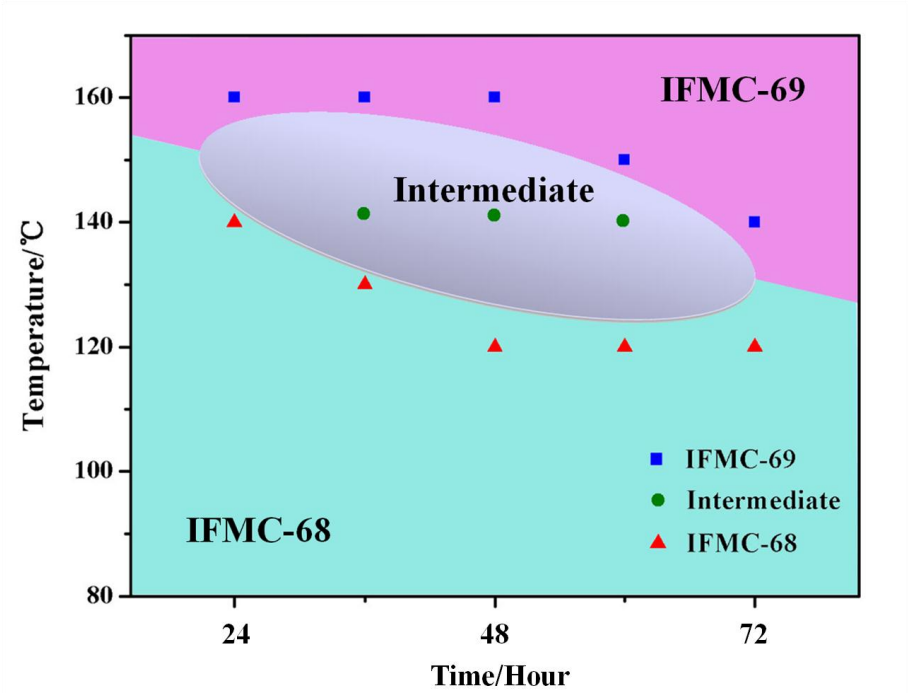

Fig. S12 The schematic distribution diagram of **IFMC-68**, intermediate and **IFMC-69** based on different time and temperatures by direct synthesis method.

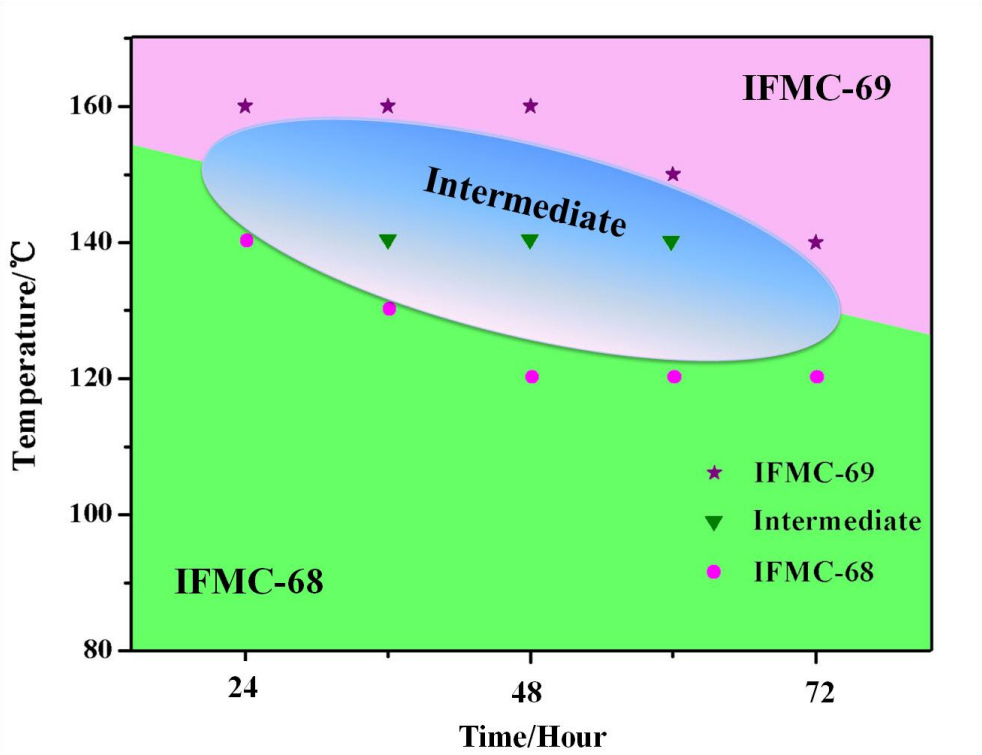

Fig. S13 The schematic distribution diagram of **IFMC-68**, intermediate and **IFMC-69** based on different time and temperatures by SCSC transformation in DMA or DMF.

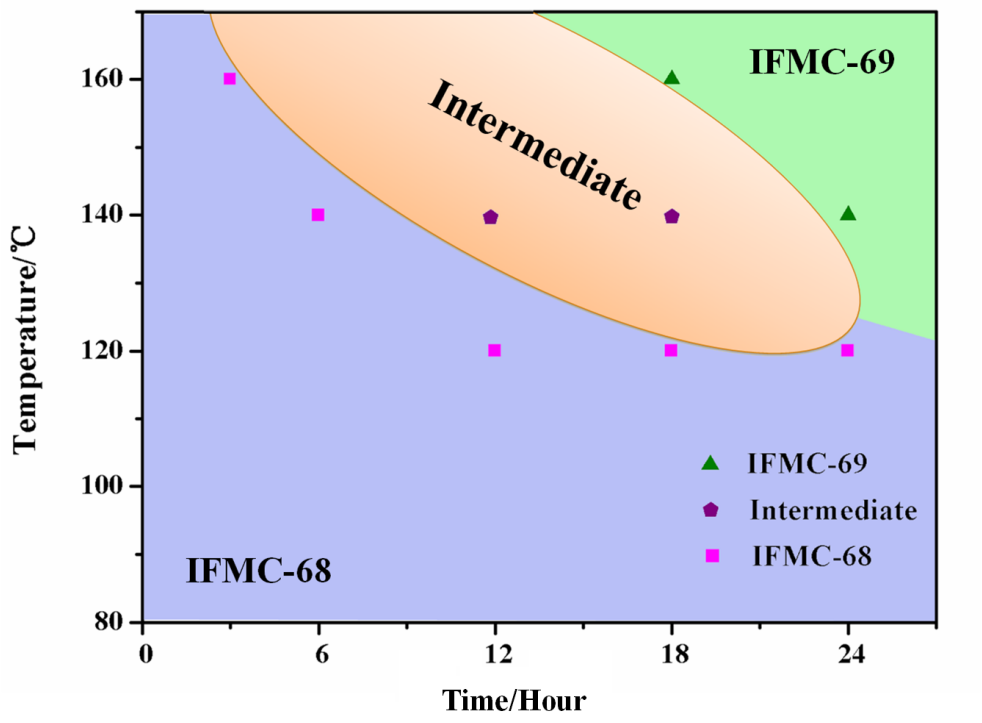

Fig. S14 The schematic distribution diagram of **IFMC-68**, intermediate and **IFMC-69** based on different time and temperatures by SCSC transformation without solvent in Teflon reactor.

Table S1 The experimental data of direct synthesis method and stepwise synthesis method based on different time and temperatures.

Synthesis Method	Solvent	Time (Hour)	Temperature				
			85℃	100℃	120℃	140℃	160℃
$H_4L+Zn(NO_3)_2$ (direct)	DMA	24				IFMC-68	IFMC-69
		48				Intermediate	IFMC-69
		72	IFMC-68	IFMC-68	IFMC-68	IFMC-69	IFMC-69
	DMF	24				IFMC-68	IFMC-69
		48			IFMC-68	Intermediate	IFMC-69
		72	IFMC-68	IFMC-68	IFMC-68	IFMC-69	IFMC-69
IFMC-68 (step-wise)	DMA	24	IFMC-68	IFMC-68	IFMC-68	IFMC-68	IFMC-69
		48	IFMC-68	IFMC-68	IFMC-68	Intermediate	IFMC-69
		72	IFMC-68	IFMC-68	IFMC-68	IFMC-69	IFMC-69
	DMF	24	IFMC-68	IFMC-68	IFMC-68	IFMC-68	IFMC-69
		48	IFMC-68	IFMC-68	IFMC-68	Intermediate	IFMC-69
		72	IFMC-68	IFMC-68	IFMC-68	IFMC-69	IFMC-69
	None	24	IFMC-68	IFMC-68	IFMC-68	IFMC-69	IFMC-69
		48	IFMC-68	IFMC-68	IFMC-68	IFMC-69	IFMC-69
		72	IFMC-68	IFMC-68	IFMC-68	IFMC-69	IFMC-69

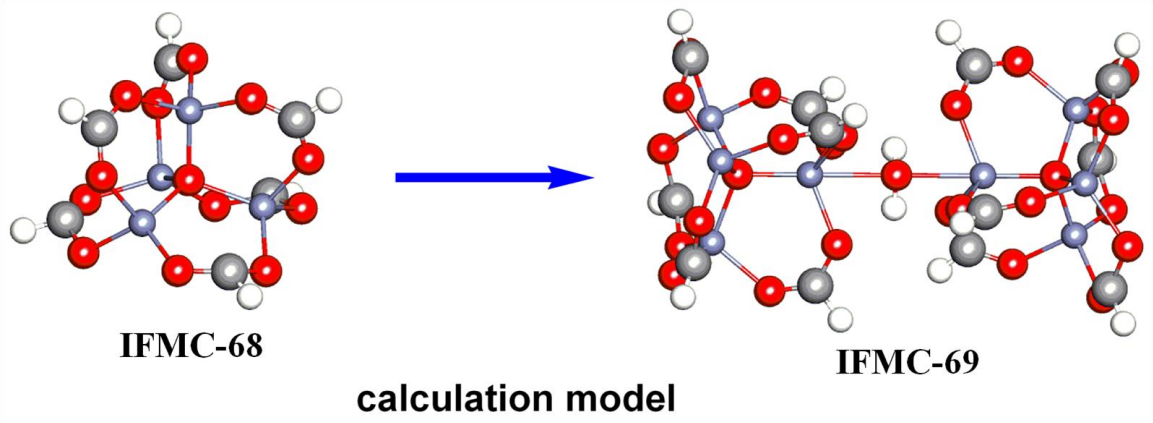

Fig. S15 The simple model of $Zn_4O(CO_2)_6$ SBU and $[Zn_4O(CO_2)_6]_2H_2O$ SBU in quantum chemical calculations.

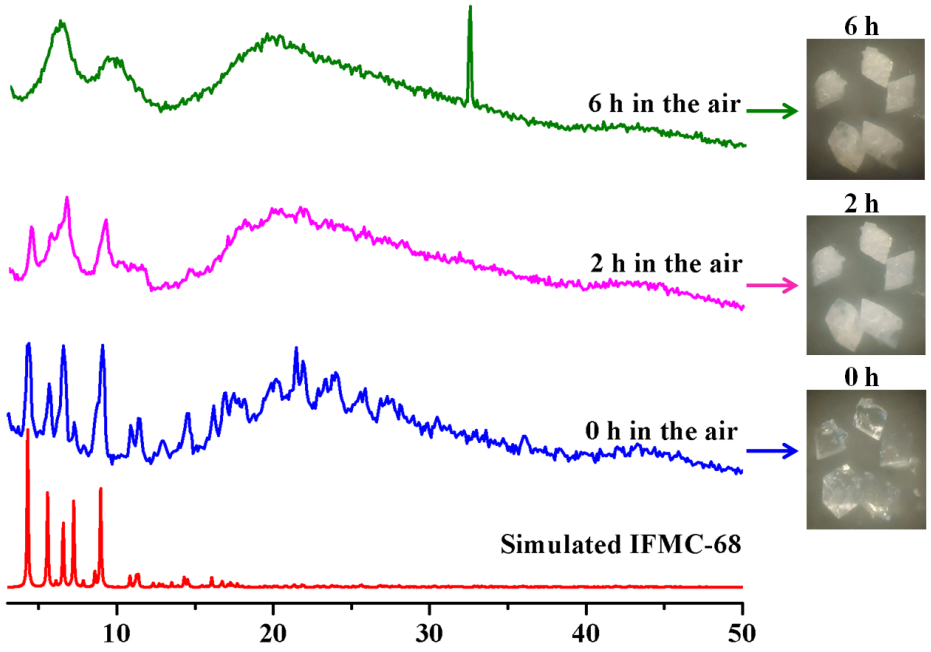

Fig. S16 X-Ray powder diffraction patterns of simulated **IFMC-68** (red), **IFMC-68** in the air for 0 h (blue), 2 h (pink) and 6 h (dark green) (left). Photos of corresponding crystals (right).

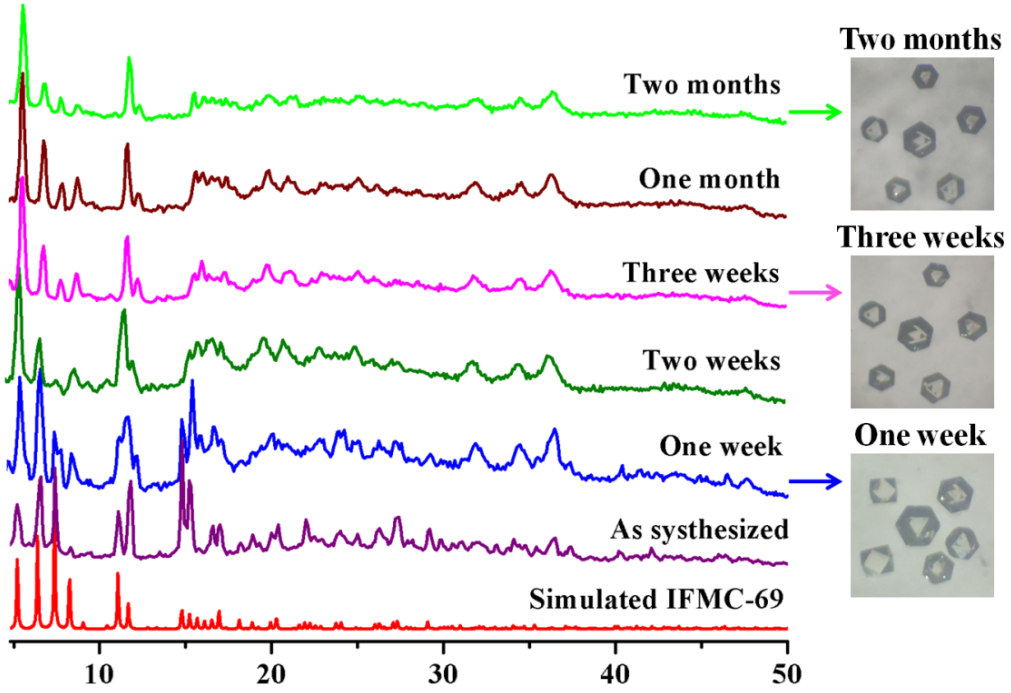

Fig. S17 X-Ray powder diffraction patterns of the simulated **IFMC-69** (red), the as-systhesized **IFMC-69** (purple), **IFMC-69** in the air for one week (blue), two weeks (dark green), three weeks (pink), one month (dark red) and two months (green) (left). Photos of corresponding crystals (right).

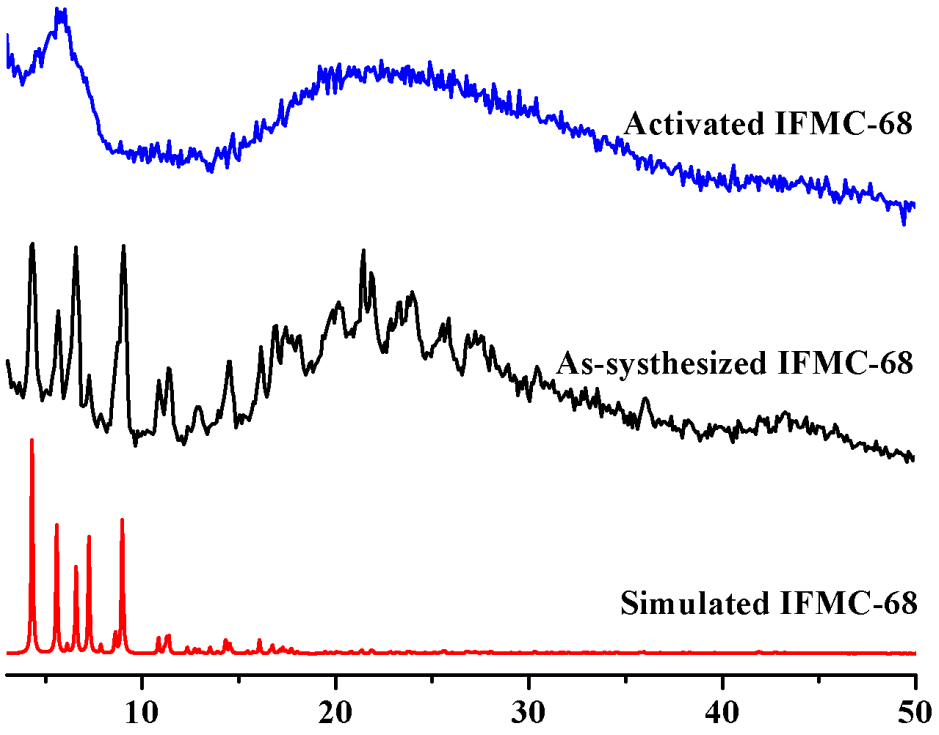

Fig. S18 X-Ray powder diffraction patterns of simulated **IFMC-68** (red), as-synthesized **IFMC-68** (black) and activated **IFMC-68** (blue).

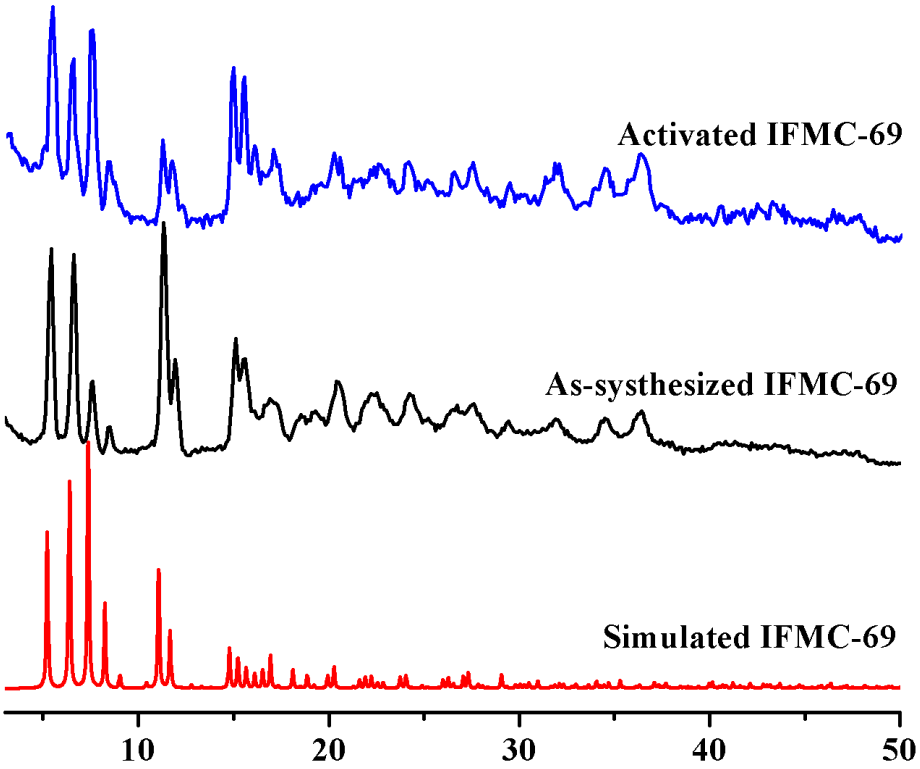

Fig. S19 X-Ray powder diffraction patterns of simulated **IFMC-69** (red), as-synthesized **IFMC-69** (black) and activated **IFMC-69** (blue).

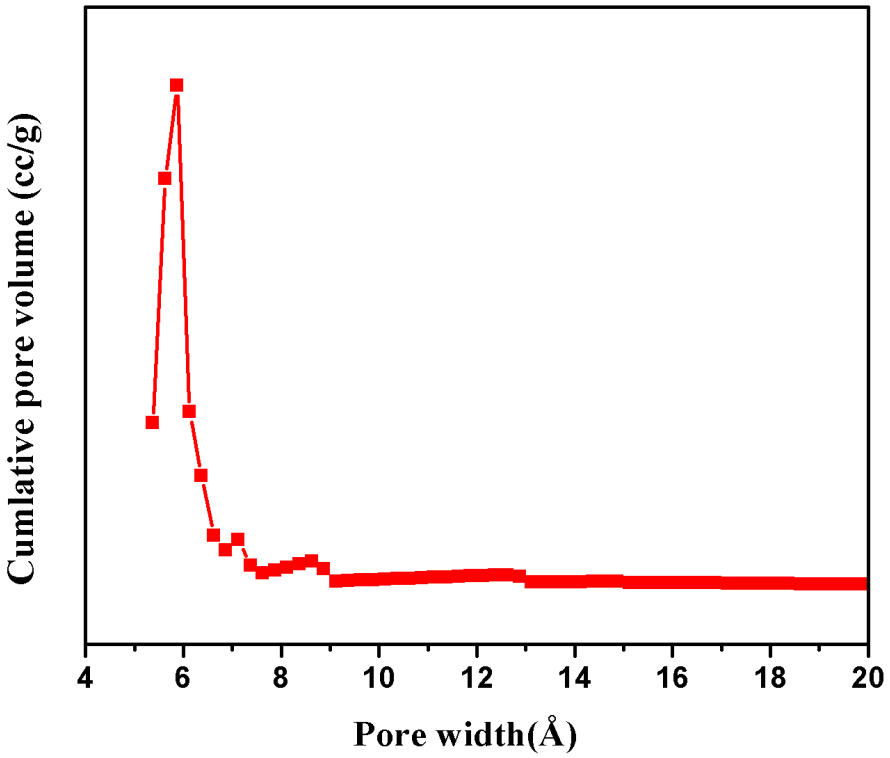

Fig. S20 The pore size distribution of **IFMC-69** based on N_2 adsorption at 77 K.

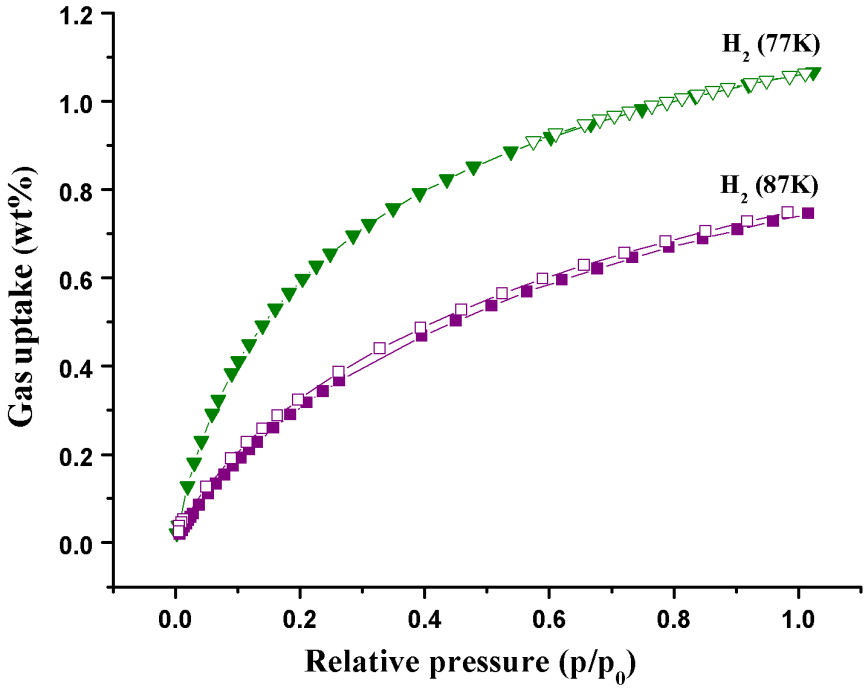

Fig. S21 The H_2 gas-sorption isotherms for **IFMC-69** at 77K (green) and 87K (purple), respectively. The filled and open squares representation of adsorption and desorption branches, respectively.

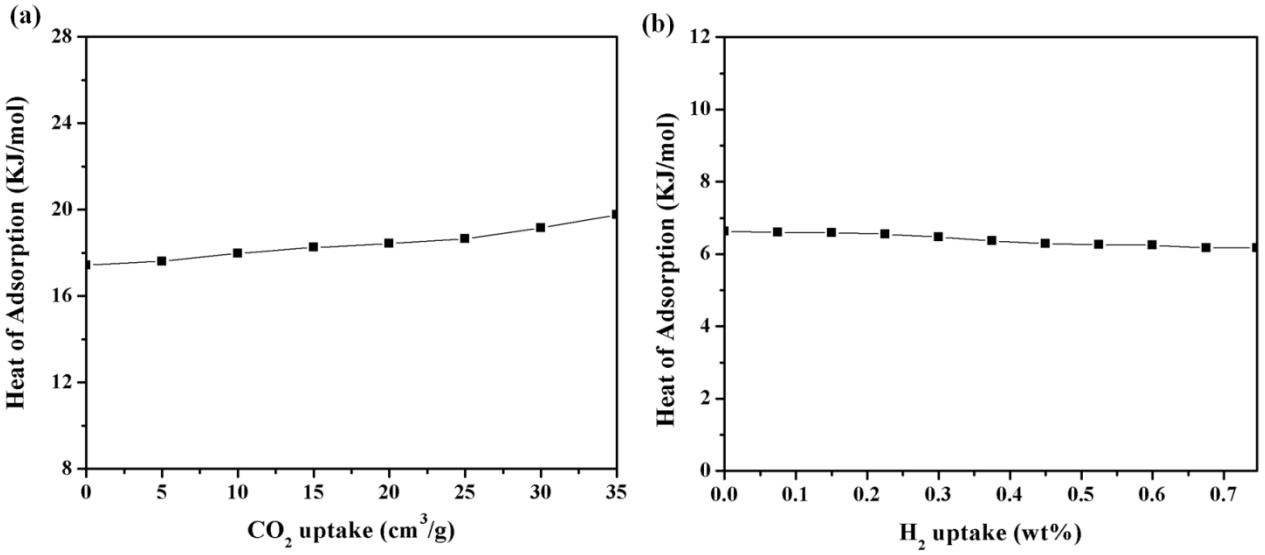

Fig. S22 (a) CO_2 heat of adsorption for **IFMC-69**. (b) H_2 heat of adsorption for **IFMC-69**.

Table S2 CO_2 and N_2 adsorption data of **IFMC-69**.

Temperature	Gas	Adsorption amount (at saturation)			Number of molecules per unit cell
		$cm^3 \cdot g^{-1}$	$mmol \cdot g^{-1}$	L/L	
273 K	CO_2	56.96	2.54	66.24	24.5
	N_2	10.92	0.49	12.70	4.7
298 K	CO_2	35.88	1.60	41.73	15.4
	N_2	1.10	0.05	1.28	0.5

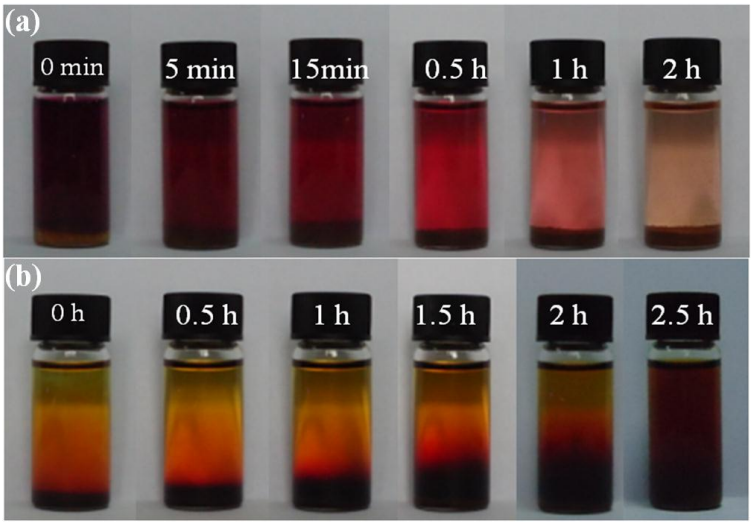

Fig. S23 (a) Photos for **IFMC-69** of adsorping I_2 process in hexane solution of I_2 (3 mL, 0.01 mol/L). (b) I_2 release process in 3 mL EtOH.

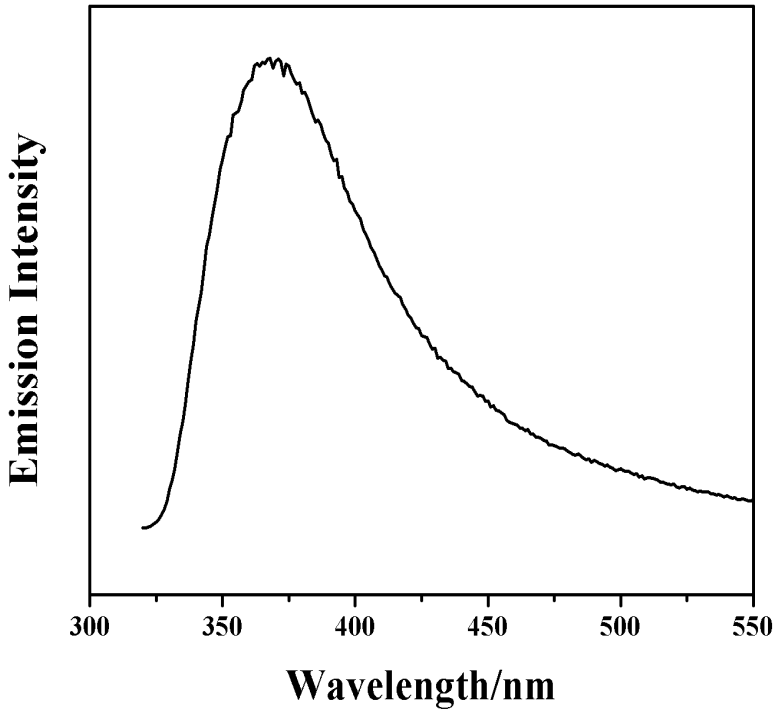

Fig. S24 Emission spectrum of **H_4L** in the solid state at room temperature.

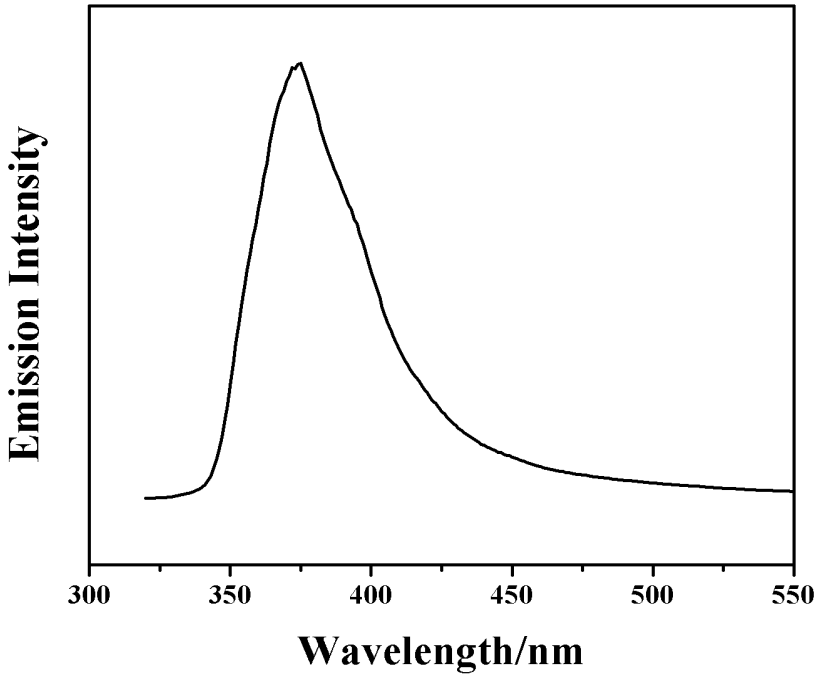

Fig. S25 Emission spectrum of **IFMC-69** in the solid state at room temperature.

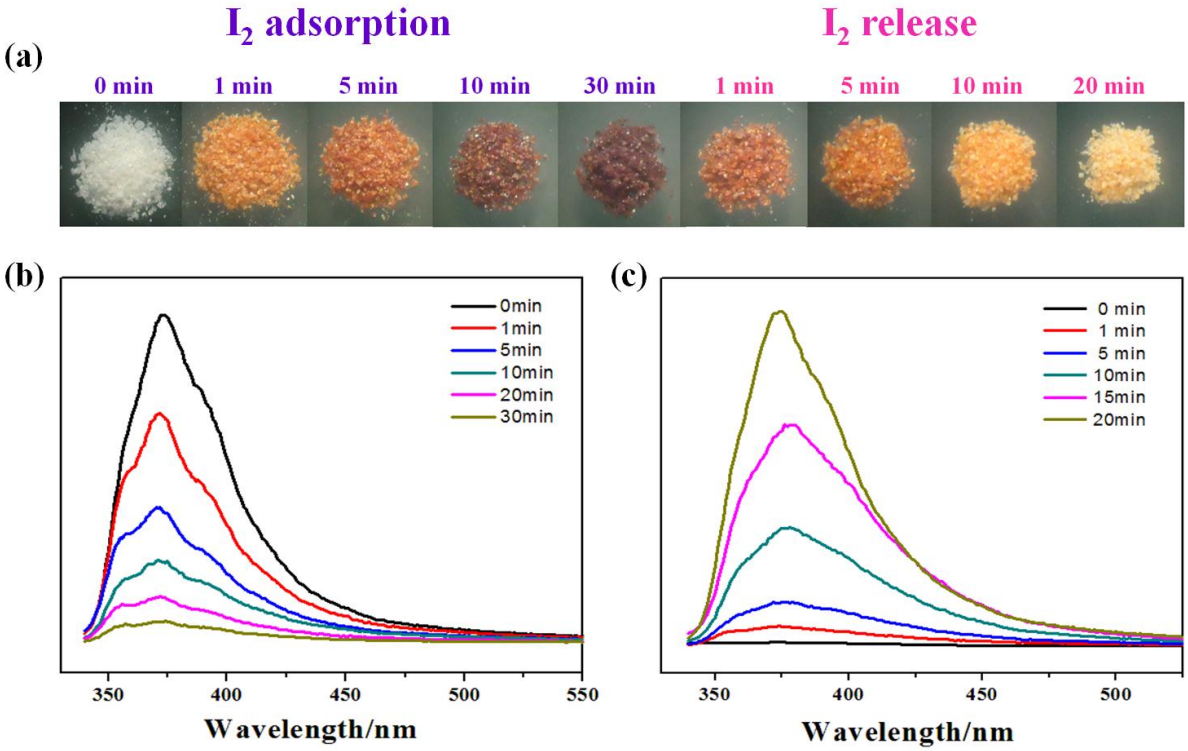

Fig. S26 (a) Photos for **IFMC-69** of I_2 adsorption (hexane) and release (ethanol). (b) Photoinduced solid state emission spectra of **IFMC-69** and **IFMC-69** in I_2 solution within 0~30 min (λex = 300 nm and λem = 374nm). (c) Photoinduced solid state emission spectra of **I_2@IFMC-69** in ethanol within 0-20 min.

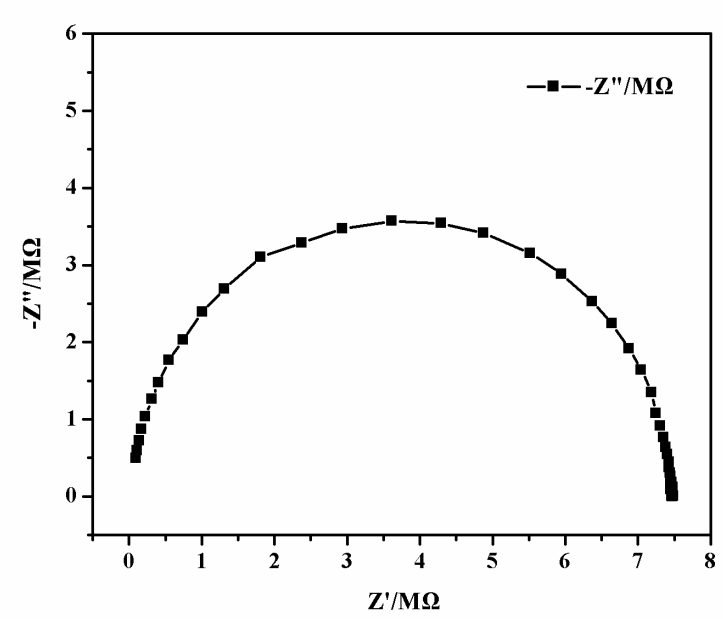

Fig. S27 Nyquist plot of **I_2@IFMC-69**.

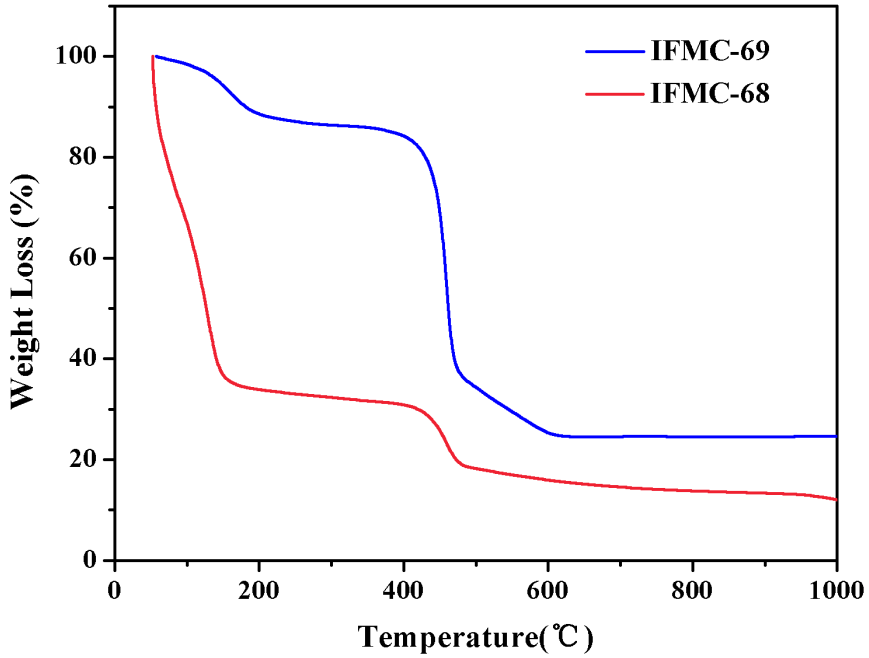

Fig. S28 TGA curves of **IFMC-68** (red) and **IFMC-69** (blue).

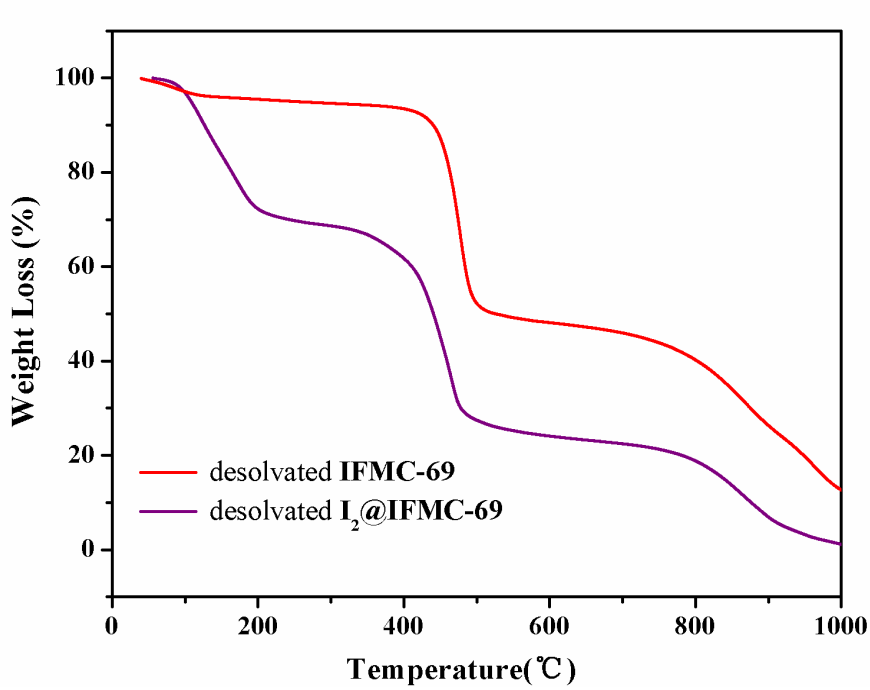

Fig. S29 TGA curves of desolvated **IFMC-69** (red, solvent was removed after soaking **IFMC-69** in hexane) and desolvated **I_2@IFMC-69** (purple, solvent was removed after immersing **IFMC-69** in a hexane solution of I_2 (0.05 mol/L) for 24 hours).

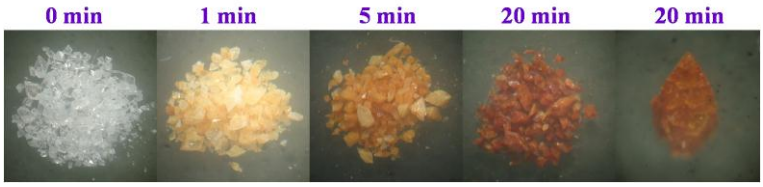

Fig. S30 Photos for **IFMC-68** of I_2 adsorption (hexane) and single crystal of **IFMC-68** whose framework partially collapsed after adsorbing I_2 for 20 minutes.

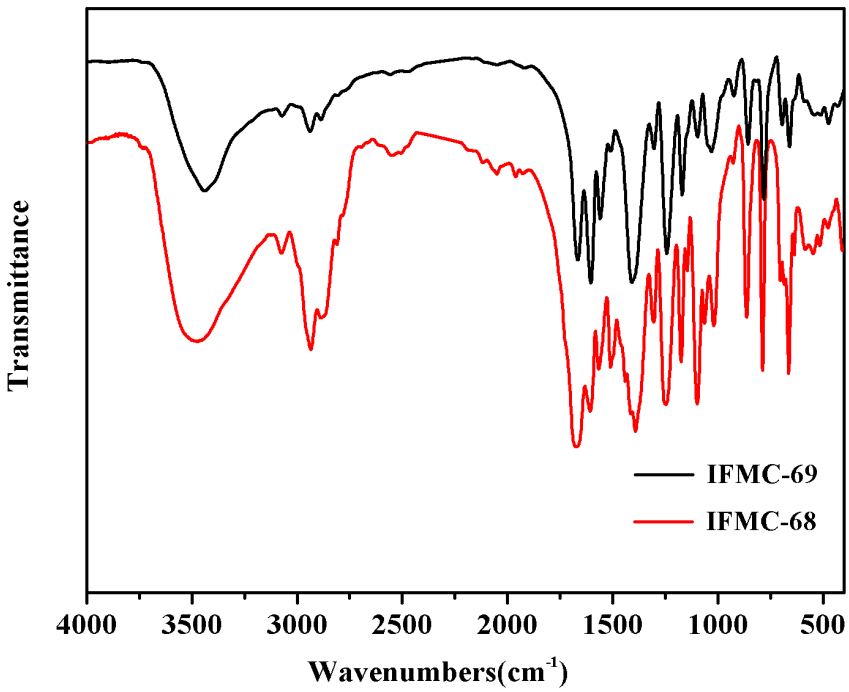

Fig. S31 IR spectra for **IFMC-68** (red) and **IFMC-69** (black).